3278 *Inorg. Chem.* **2010**, *49*, 3278–3281
DOI: 10.1021/ic902148y

Inorganic Chemistry
Article

Theoretical Revisit of a $Fe(CO)_5$-Catalyzed Water−Gas Shift Reaction

Fuli Zhang, Liang Zhao, Chunming Xu, and Yu Chen*

State Key Laboratory of Heavy Oil Processing, China University of Petroleum, Changping, Beijing 102249, People's Republic of China

Received October 30, 2009

We have revisited the water−gas shift reaction catalyzed by iron pentacarbonyl at the DFT-B3LYP level. The reaction mechanism proposed by Rozanska and Vuilleumier (*Inorg. Chem.* **2008**, *47*, 8635−8640) has been followed and revised. The results show that transition states **TS4/5** and **TS5/2_a** actually connect other intermediates rather than those suggested by Rozanska and Vuilleumier. Furthermore, the entire reaction has been proven to proceed with processes **1** → **2** → **3** → **4** → **6** → **7** → **2**. It is the first time that species **6** and **7** are reported as intermediates for this reaction mechanism.

Introduction

The water−gas shift reaction (WGSR), eq 1, plays an important role in the chemical industry worldwide. It can be used to regulate the CO/H_2 molar ratio in synthesis gas and in fuel cells.

$$CO(g) + H_2O(g) \rightarrow H_2(g) + CO_2(g) \qquad (1)$$

Homogeneous catalysis of the WGSR by transition-metal carbonyls has attracted considerable attention because of its mild conditions. Among all of those homogeneous catalysts, iron pentacarbonyl is often chosen to extensively analyze the reaction mechanisms experimently.[1,2] After extensive investigation, Sunderlin and Squires[3] postulated a $Fe(CO)_5$-catalyzed WGSR catalytic cycle based on experimental results, where species $Fe(CO)_4$, $(CO)_4FeH^-$, and $(CO)_4FeH_2$ were included as intermediates. Torrent and co-workers[4] precisely inspected Sunderlin and Squires' mechanism by means of theoretical methods and proposed a more detailed mechanism as shown in Scheme 1.

In that catalytic cycle, the OH^- desorption from an iron complex is, however, very energy-demanding, with an enthalpy change of $\Delta H = 308$ kJ/mol in the gas phase, which makes Scheme 1 unlikely to proceed, partly or entirely. In view of that reason, Barrows[5] presented an associative reaction mechanism where no OH^- desorption was required (Scheme 2).

Nevertheless, the catalytic cycle in Scheme 2 is still not perfect because the experimentally observed $(CO)_4FeH^-$ was not included. After a systematical analysis of the gas-phase mechanisms in basic conditions, Rozanska and Vuilleumier (RV)[6] developed a novel mechanism. This mechanism not only included species $(CO)_4FeH^-$ but also excluded the energy-demanding OH^- desorption, which made the reaction cycle impossible (Scheme 3).

Although the mechanism in Scheme 3 seems to have explained all observations, other paths are still possible. To get more details and to facilitate a comparison with corresponding complexes of other members in the iron group, i.e., $Ru(CO)_5$ and $Os(CO)_5$, we decided to revisit the iron pentacarbonyl catalyzed reaction mechanism.

We recalculated the reaction pathways proposed by RV.[6] The calculation results indeed showed a new transition state. Extended investigations indicated that the transition states **TS4/5** and **TS5/2_a** provided by RV[6] should connect other intermediates rather than those proposed. In this study, we describe the reaction mechanism in detail.

Theoretical Methods

All reactions in Scheme 3 were traced carefully by using the Frenking group's standard basis set II,[7] which is the same as that which Torrent et al.[4] applied for the WGSR. This basis set uses a small-core effective core potential with a (441/2111/41) valence basis set for the Fe atom and 6-31G(d,p) basis sets for other atoms. Our previous works[8,9] demonstrated that

*To whom correspondence should be addressed. E-mail: chenyu@cup.edu.cn.

(1) Brice, N.; Kao, S. C.; Pettit, R. *J. Am. Chem. Soc.* **1979**, *101*, 1627.
(2) Lane, K. R.; Lee, R. E.; Sallans, L.; Squires, R. R. *J. Am. Chem. Soc.* **1984**, *106*, 5767.
(3) Sunderlin, L. S.; Squires, R. R. *J. Am. Chem. Soc.* **1993**, *115*, 337.
(4) Torrent, M.; Solà, M.; Frenking, G. *Organometallics* **1999**, *18*, 2801.
(5) Barrows, S. E. *Inorg. Chem.* **2004**, *43*, 8236.
(6) Rozanska, X.; Vuilleumier, R. *Inorg. Chem.* **2008**, *47*, 8635.
(7) Frenking, G.; Antes, I.; Böhme, M.; Dapprich, S.; Ehlers, A. W.; Jonas, V.; Neuhaus, A.; Otto, M.; Stegmann, R.; Veldkamp, A.; Vyboishchikov, S. F. In *Reviews in Computational Chemistry*; Lipkowitz, K. B., Boyd, D. B., Eds.; VCH: New York, 1996; Vol. *8*, pp 63−144.
(8) Chen, Y.; Petz, W.; Frenking, G. *Organometallics* **2000**, *19*, 2698.
(9) Chen, Y.; Hartmann, M.; Frenking, G. *Z. Anorg. Allg. Chem.* **2001**, *627*, 985.

 Published on Web 03/02/2010

Scheme 1. Mechanism Proposed by Torrent et al. for a $Fe(CO)_5$-Catalyzed WGSR

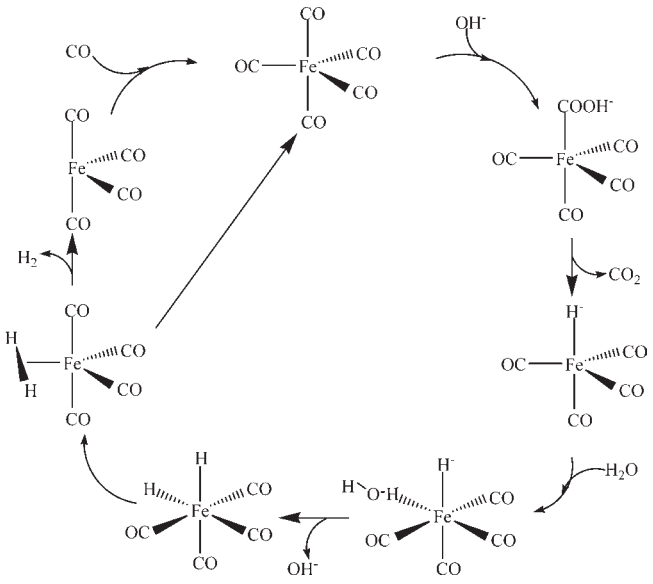

Scheme 2. Mechanism Proposed by Barrows for a $Fe(CO)_5$-Catalyzed WGSR

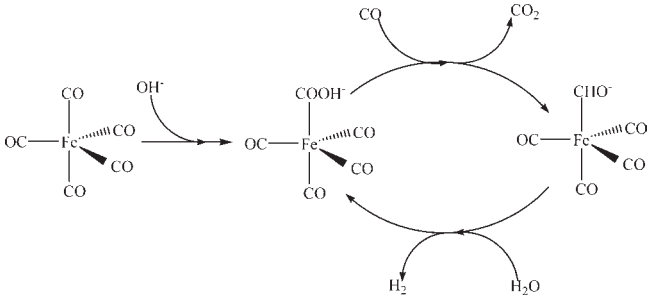

Scheme 3. Mechanism Proposed by Rozanska and Vuilleumier for a $Fe(CO)_5$-Catalyzed WGSR

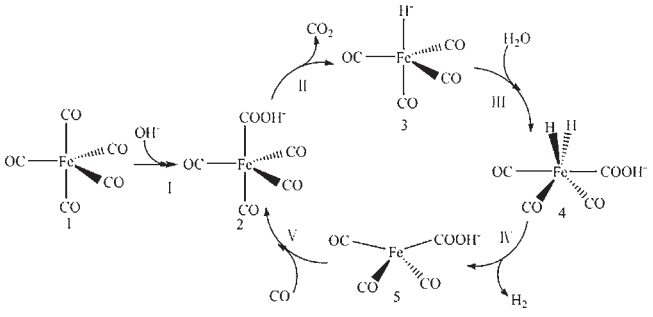

this basis set can very well reproduce the structures of transition-metal complexes, such as $Fe(CO)_4L$, where L stands for a series of ligands. Geometrical optimizations and vibrational frequency calculations were performed at the level of DFT-B3LYP[10] in *Gaussian 03*.[11] An extra f function[12] was added to the Fe atom for a better description. Single-point energy calculations of B3LYP/II-optimized geometries were carried out at the B3LYP level with a larger basis set II++ for all reaction steps involved in the reaction mechanism. II++ is the same as II plus the addition of diffuse functions for C, H, and O atoms, i.e., using 6-31++G(d,p). All energy values are given at the B3LYP/II++//B3LYP/II level with zero-point energy (ZPE) corrections.

Results and Discussion

Figure 1 displays our calculated energy profile for the $Fe(CO)_5$-catalyzed WGSR.

Obviously, the first half of this reaction cycle, namely, **1** → **2** → **3** → **4** (Figure 1a and Scheme 3), is consistent with RV's conclusion.[6] Differences appear regarding how compound **4** evolves back to compound **2** to complete the reaction cycle.

According to RV,[6] complex $FeH_2(CO)_3COOH^-$ (**4**) transformed to $Fe(CO)_3COOH^-$ (**5**) via transition state **TS4/5** and then to $Fe(CO)_4COOH^-$ (**2**) via **TS5/2_a**. However, as we can see from Figure 2, **5**, **2**, and **TS5/2_a** have different relative configurations with respect to the COOH group. In **TS5/2_a**, the H atom syn to C=O in the COOH group is far away from the Fe atom and equatorial CO groups. In contrast, in both **5** and **2**, this H atom is anti to C=O in the COOH group and adjacent to the iron carbonyl fragment. This means that for the process of **5** → **2** the COOH group has to undergo a configurational or conformational change twice, through either H migration or H rotation. This change might be possible but is surely difficult[13] and indirect. The process **TS4/5**→**5** is also. Thus, there should be some other paths or intermediates. Just as anticipated, we localized a new transition state structure **TS5/2_b**. This find seemed to have shed light on a possible solution for the aforementioned problem because **TS5/2_b** is calculated to be 8.4 kJ/mol lower in energy than RV's type[6] **TS5/2_a**. Besides that, the relative configuration of carboxyl for the transition state **TS5/2_b** is obviously similar to that of both reactant **5** and product **2**, and the bond length of the C−O single bond in the COOH group (1.378 Å) is reasonably just between that of reactant **5** (1.374 Å) and product **2** (1.392 Å). Nonetheless, replacing **TS5/2_a** with **TS5/2_b** alone is still not enough to perfect the reaction mechanism. Therefore, we shifted focus from the process **5** → **2** to the more complicated process **4** → **2**, which might, but not necessarily, include **5** → **2**. We found three routes for the change of **4** → **2** (Figure 1b): route A (**4** → **6** → **7** → **2**), route B (**4** → **6** → **8** → **5** → **2**), and route C (**4** → **9** → **10** → **5** → **2**). It is obvious that **4** → **5** is not a single step but a three-step process. One step is dehydrogenation, and the other two are conformational changes by H rotation around the C−O single bond and configurational conversion through H transfer in the COOH group, respectively. What is interesting is that, out of the three competing paths, route A is the only one that contains no intermediate **5**

(10) Becke, A. D. *J. Chem. Phys.* **1993**, *98*, 5648. Lee, C.; Yang, W.; Parr, R. G. *Phys. Rev.* **1988**, *B37*, 785.

(11) Frisch, M. J.; Trucks, G. W.; Schlegel, H. B.; Pople, J. A.; et al. *Gaussian 03*, revision E.01; Gaussian, Inc.: Wallingford, CT, **2004**. See the Supporting Information for the full citation.

(12) Ehlers, A. W.; Böhme, M.; Dapprich, S.; Gobbi, A.; Höllwarth, A.; Jonas, V.; Köhler, K. F.; Stegmann, R.; Veldkamp, A.; Frenking, G. *Chem. Phys. Lett.* **1993**, *208*, 111.

(13) Additional calculations show that extra energy is required for both rotational isomerization and migration of the H atom of the COOH group in the iron carbonyl complexes. To activate an anti−syn isomerization, **5** → **8**, it costs 43.7 kJ/mol (see Figure 1b and the Supporting Information). The H migration will be even more difficult to perform because the energy barrier is predicted to be 98.8 kJ/mol for **8** → **6**. Note that the calculated energy barriers for cis−trans transformation (rotational isomerization) and trans−trans conversion (H transfer) in HCOOH are 25.7 and 127.5 kJ/mol, respectively.

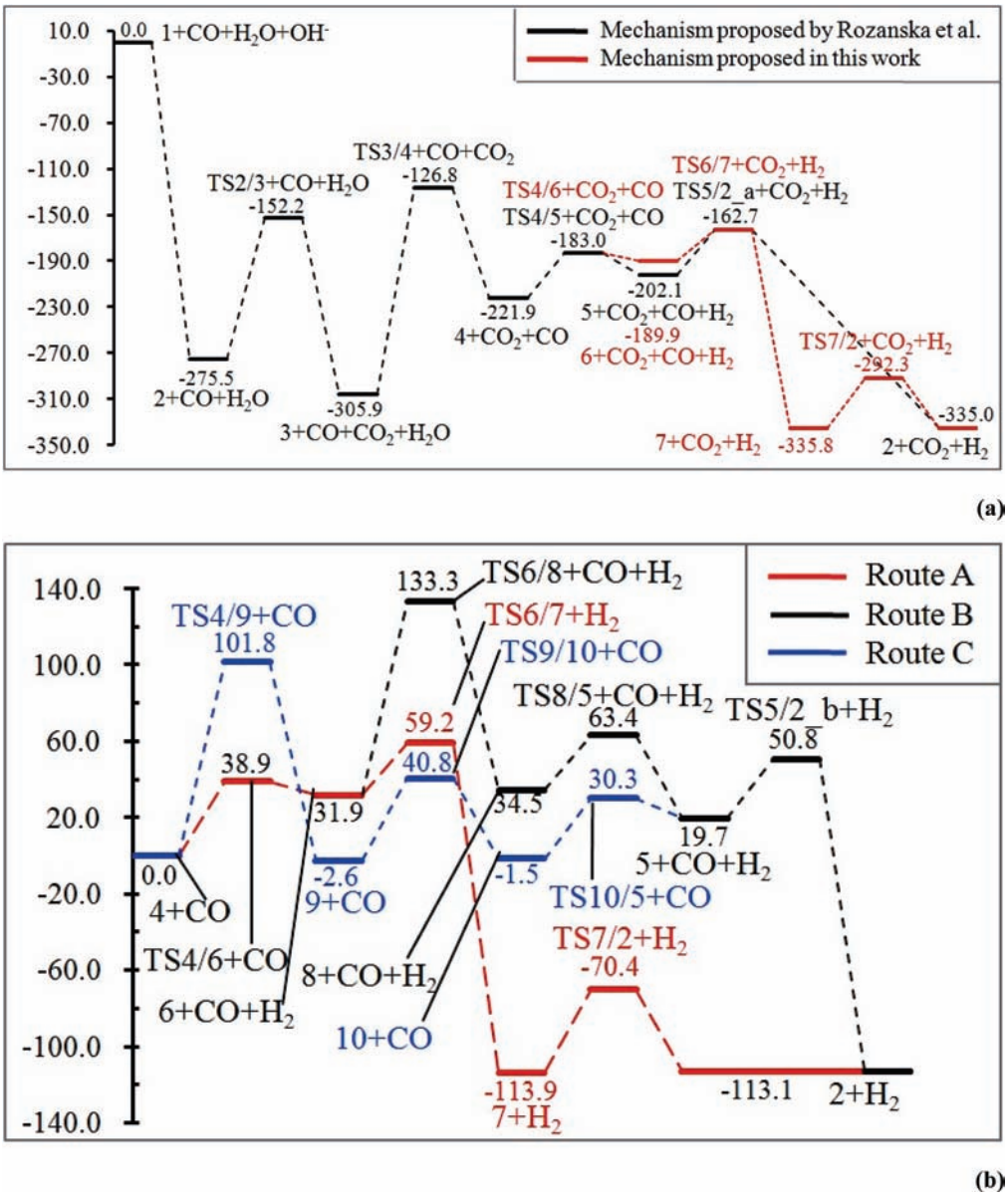

Figure 1. Energy profile of the gas-phase WGSR catalyzed by $Fe(CO)_5/OH^-$ in Scheme 3, calculated at the level of B3LYP/II++ including ZPE contributions at the level of B3LYP/II (in kJ/mol).

but is still the most favorable one! For this reason, in Figure 3, only structures related to route A are displayed. The other geometry structures are shown in the Supporting Information.

Figures 1 and 3 show that the intermediate **4** can directly change into **6** through dehydrogenation, followed by the formation of **7** via coordination of CO to **6**. Finally **7** transforms into **2** by H rotation around the C−O bond of the COOH group. Characterizations of the transition states by means of intrinsic reaction coordinate calculations has verified that **TS4/6**, **TS6/7**, and **TS7/2** are all correct transition states that link individual reaction partners directly. Surprisingly, the structure of **TS4/6** is fully identical with that of **TS4/5**, while the structure of **TS6/7** is the same as that of **TS5/2_a**. That is to say, it is not **5** but its isomer **6** on the product side of **TS4/6** or **TS4/5**, although **6** is 12.2 kJ/mol less stable than **5** (see Figure 1a). As for **TS5/2_a** or exactly **TS6/7**, the situation is even more interesting because it actually connects the intermediates **6** and **7**. The follow-up conversion from **7** to **2** via **TS7/2** can take place easily with an energy barrier of 43.5 kJ/mol, releasing CO_2 and H_2.

So far, the configurational changes of the COOH group for those structures involved in the reaction mechanism are reasonably clarified. The reaction cycle should be as follows: processes **1** → **2** → **3** → **4** followed by pathways **4** → **6** → **7** → **2**. Our ongoing theoretical investigations of the WGSR with ruthenium- and osmium-based catalysts will provide more insight into the mechanism of this reaction.

Conclusions

Our calculation results show that **TS5/2_a** proposed by RV[6] does not connect **5** and **2** directly. It actually connects new intermediates **6** and **7**, which are reported for the first time. The single-step reaction **4** → **5** cannot take place as suggested by RV[6] because there are two other intermediates in this transformation process. In addition, neither of the two routes that include **5**, namely, route B (**4** → **6** → **8** → **5** → **2**)

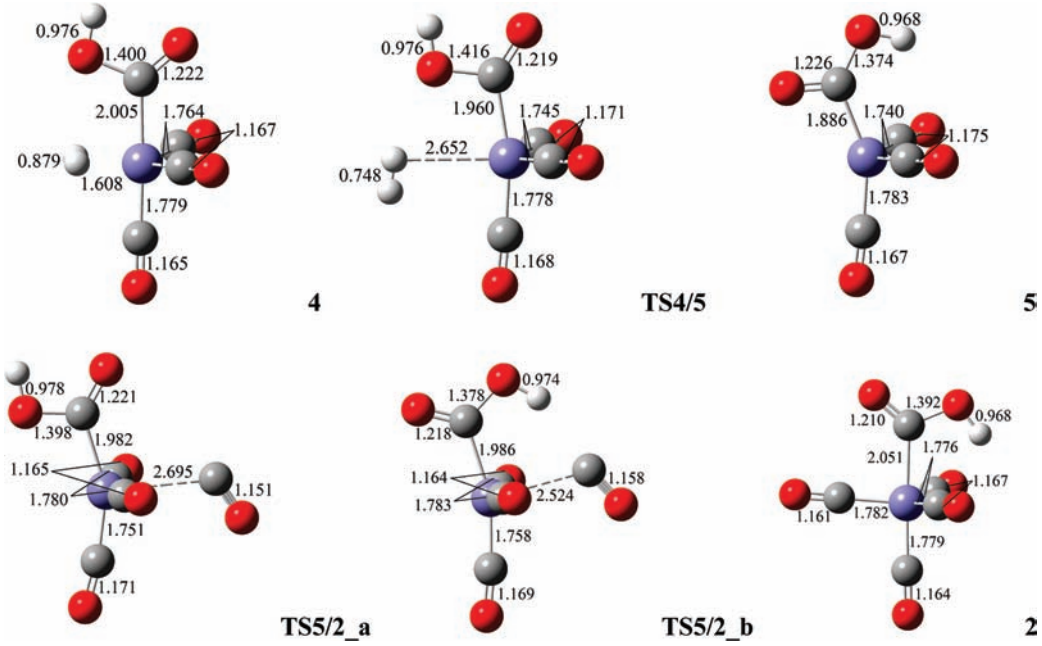

Figure 2. Optimized geometries of **4**, **5**, **2**, **TS4/5**, **TS5/2_a**, and **TS5/2_b**. Bond distances are given in angstroms.

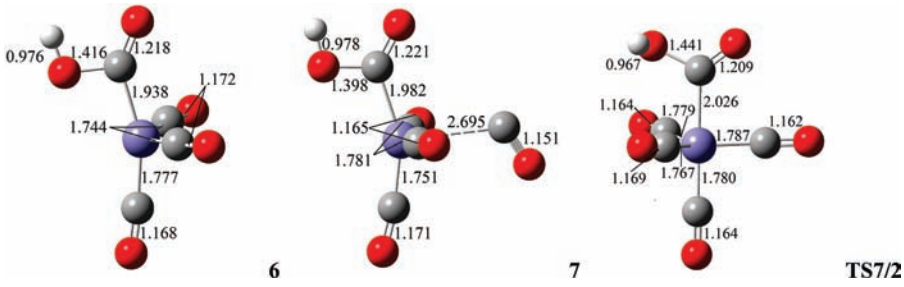

Figure 3. Optimized geometries of **6**, **7**, and **TS7/2**. The bond distances are given in angstroms.

and route C (**4** → **9** → **10** → **5** → **2**), is favorable in energy. The reaction may proceed with sequence **1** → **2** → **3** → **4** → **6** → **7** → **2** via **TS4/6** and **TS6/7**.

Acknowledgment. We thank all anonymous reviewers for valuable comments concerning the earlier version. This work is supported by the National Natural Science Foundation of China (Grants 20873180 and 20525621), the Scientific Research Foundation for the Returned Overseas Chinese Scholars by Ministry of Education, and the Program of the State Key Laboratory of Heavy Oil Processing (Grants 2006-4 and 2008-4).

Supporting Information Available: Optimized geometries (Figure S1), calculated total energies and ZPEs at the B3LYP/II level and single-point energy energies at the B3LYP/II++ level (Table S1), and complete ref 11. This material is available free of charge via the Internet at http://pubs.acs.org.